European Radiology (2022) 32:2437–2447
https://doi.org/10.1007/s00330-021-08337-3

GASTROINTESTINAL

Comparison of metabolic and immunologic responses to transarterial chemoembolization with different chemoembolic regimens in a rabbit VX2 liver tumor model

Luzie A. Doemel[1,2] · Jessica G. Santana[1] · Lynn J. Savic[1,2,3] · Fabian M. Laage Gaupp[1] · Tabea Borde[1,4] · Alexandra Petukhova-Greenstein[1,2] · Ahmet S. Kucukkaya[1,2] · Isabel T. Schobert[1,2] · Charlie A. Hamm[2,5] · Bernhard Gebauer[2] · John J. Walsh[6] · Irvin Rexha[1,2] · Fahmeed Hyder[1,6,7] · MingDe Lin[1,8] · David C. Madoff[1,7,9,10,11] · Todd Schlachter[1] · Julius Chapiro[1,7] · Daniel Coman[1,7]

Received: 13 March 2021 / Revised: 12 August 2021 / Accepted: 9 September 2021 / Published online: 31 October 2021

Abstract

Objectives The goal of this study was to investigate the effects of TACE using Lipiodol, Oncozene™ drug-eluting embolics (DEEs), or LUMI™-DEEs alone, or combined with bicarbonate on the metabolic and immunological tumor microenvironment in a rabbit VX2 tumor model.

Methods VX2 liver tumor-bearing rabbits were assigned to five groups. MRI and extracellular pH (pH_e) mapping using Biosensor Imaging of Redundant Deviation in Shifts (BIRDS) were performed before and after intra-arterial therapy with conventional TACE (cTACE), DEE-TACE with Idarubicin-eluting Oncozene™-DEEs, or Doxorubicin-eluting LUMI™-DEEs, each with or without prior bicarbonate infusion, and in untreated rabbits or treated with intra-arterial bicarbonate only. Imaging results were validated with immunohistochemistry (IHC) staining of cell viability (PCNA, TUNEL) and immune response (HLA-DR, CD3). Statistical analysis was performed using Mann–Whitney *U* test.

Results pH_e mapping revealed that combining cTACE with prior bicarbonate infusion significantly increased tumor pH_e compared to control ($p=0.0175$) and cTACE alone ($p=0.0025$). IHC staining revealed peritumoral accumulation of HLA-DR$^+$ antigen-presenting cells and CD3+T-lymphocytes in controls. cTACE-treated tumors showed reduced immune infiltration, which was restored through combination with bicarbonate. DEE-TACE with Oncozene™-DEEs induced moderate intratumoral and marked peritumoral infiltration, which was slightly reduced with bicarbonate. Addition of bicarbonate prior to LUMI™-beads enhanced peritumoral immune cell infiltration compared to LUMI™-beads alone and resulted in the strongest intratumoral immune cell infiltration across all treated groups.

Conclusions The choice of chemoembolic regimen for TACE strongly affects post-treatment TME pH_e and the ability of immune cells to accumulate and infiltrate the tumor tissue.

Key Points

- *Combining conventional transarterial chemotherapy with prior bicarbonate infusion increases the pH_e towards a more physiological value ($p=0.0025$).*
- *Peritumoral infiltration and intratumoral accumulation patterns of antigen-presenting cells and T-lymphocytes after transarterial chemotherapy were dependent on the choice of the chemoembolic regimen.*
- *Combination of intra-arterial treatment with Doxorubicin-eluting LUMI™-beads and bicarbonate infusion resulted in the strongest intratumoral presence of immune cells (positivity index of 0.47 for HLADR$^+$-cells and 0.62 for CD3$^+$-cells).*

Keywords Carcinoma, hepatocellular · Tumor microenvironment · Chemoembolization, therapeutic · Rabbits · Immunohistochemistry

Abbreviations

APC	Antigen-presenting cells
BIRDS	Biosensor Imaging of Redundant Deviation in Shifts
cTACE	Conventional TACE
DEE-TACE	TACE with drug-eluting embolics
HCC	Hepatocellular carcinoma
IHC	Immunohistochemistry

Luzie A. Doemel and Jessica G. Santana contributed equally to this work and therefore share first authorship

Julius Chapiro and Daniel Coman shared contribution as senior authors

Extended author information available on the last page of the article

pH_e	Extracellular pH
PI	Positivity index
TACE	Transarterial chemoembolization
TME	Tumor microenvironment

Introduction

Hepatocellular carcinoma (HCC) is the third most common cause of cancer-related death worldwide and is often diagnosed late, rendering curative treatment options no longer applicable [1, 2]. Patient survival with intermediate stage HCC classified as Barcelona Clinic Liver Cancer B [3] is improved by transarterial chemoembolization (TACE) as shown in multiple randomized controlled trials [4–6]. A broad variety of chemoembolic regimens is available for TACE. Most commonly, conventional TACE (cTACE) is applied, which uses selective arterial injection of a water-in-oil emulsion of chemotherapeutics and Lipiodol into tumor-feeding arteries resulting in high intratumoral concentration of the chemotherapeutic agent and, if followed by embolization, instant tumor necrosis [7]. In recent years, TACE using drug-eluting embolics (DEE-TACE) was introduced as alternative to cTACE, facilitating a slower intratumoral release of the chemotherapeutic drug, leading to a decrease of adverse events [8, 9]. Various DEE-TACE platforms have been introduced, such as Polyzene®-F-coated Oncozenes™ (Varian Medical Systems) or radiopaque LUMI™-beads (Boston Scientific). Comparisons of efficacies, clinical outcomes, and safety between cTACE and DEE-TACE have been the subject of numerous studies, but no clear superiority has been reported [8, 10–12].

The interplay between metabolic and immunological changes after TACE has barely been investigated to date. In addition to necrosis-inducing effects, TACE has demonstrated modulating effects on the tumor microenvironment (TME) with regard to extracellular pH (pH_e) and the composition of surrounding immune cells [13]. Liver tumors often manifest a hyperglycolytic metabolic phenotype that results in the extracellular accumulation of lactate and protons resulting in an acidification of the TME. The resulting low pH has been identified as a driving factor promoting tumor proliferation, neoangiogenesis, and immune escape [14–16]. Recent investigations using the novel pH_e mapping technique Biosensor Imaging of Redundant Deviation in Shifts (BIRDS) [17, 18] demonstrated the capacity of cTACE to increase pH_e towards a more physiological level and established extracellular pH as a functional biomarker of treatment-induced metabolic changes [13]. Furthermore, the injection of sodium bicarbonate prior to cTACE revealed to restore peritumoral immune cell infiltration [19]. Several studies indicated that TACE alone induces tumor-antigen-specific T-cell-driven immune response [20, 21], associated with favorable patient survival [22]. However, differences in immune-modulating effects between different TACE regimens remain understudied. Given the heterogeneity of the disease in clinical populations and the many ongoing and planned clinical trials combining various TACE regimens with immunotherapy, a better understanding of the immunogenicity and other TME alterations caused by the different embolic vehicles used is necessary.

This study aims to investigate the effect of TACE using Lipiodol, Oncozene™-DEEs, or radiopaque LUMI™-DEEs, tested alone or in combination with sodium bicarbonate, on metabolic and immunological response of the TME in a rabbit VX2 liver tumor model.

Methods

VX2 rabbit liver tumor model

Male, treatment-naïve New Zealand White rabbits (Charles River Laboratories; weight 2.5–4 kg) were included and used under institutionally approved animal care and use committee protocols (Yale University IACUC, license number 16-R-0001, protocol number 2016–20,100). Implementation of VX2 tumor chunks into the left liver lobe was performed as previously described [11, 17, 21, 22]. Tumor growth was monitored using MRI ($n = 18$) or CT ($n = 3$) until size reached about 2 cm after 14–21 days. Rabbits with a well-demarcated solitary tumor of sufficient size either underwent treatment or served as control.

Prior to all surgical interventions, intramuscular injection of acepromazine 0.25–1 mg/kg and ketamine hydrochloride 30–45 mg/kg was used to sedate animals and analgesic buprenorphine 0.02–0.05 mg/kg as well as meloxicam 0.3 mg/kg was injected subcutaneously before and after surgical interventions. For surgeries and MRI procedures, general anesthesia was performed using isoflurane 1–3% in oxygen. To prevent hypothermia, a heat support was provided and vital parameters such as oxygen saturation, heart rate, and body temperature were monitored during experimental procedures.

Experimental study design

Twenty-one VX2 tumor-bearing rabbits were randomly assigned to five different groups (Fig. 1) undergoing multiparametric MRI to non-invasively monitor the TME pH_e as follows: (a) before treatment (control, $n = 3$), and 24 h after intra-arterial therapy with (b) cTACE without ($n = 3$) and with ($n = 3$) prior bicarbonate infusion, (c) TACE with Idarubicin-eluting Oncozene™-microspheres without ($n = 3$) and with ($n = 2$) prior bicarbonate infusion, (d) TACE with radiopaque, Doxorubicin-eluting LUMI™-beads without

($n=2$) and with ($n=2$) prior bicarbonate infusion, or (e) intra-arterial bicarbonate infusion only ($n=3$). The random numbers were generated using the standard = RAND () function in Microsoft Excel. Subsequent to post-treatment MRI, the animals were euthanized and tumor tissue was harvested for immunohistochemistry (IHC) characterization of therapy-induced immune response. We chose to perform the current experiments at 1 day after TACE to investigate the immediate effects on the TME. The long-term TACE effects (at 1 and 2 weeks) will be investigated in the future and presented in a separate paper.

Transarterial chemoembolization

A blunt dissection was performed in anesthetized rabbits to gain access to the right or left common femoral artery. A 3-French vascular sheath (Cook Medical) was placed and a 2-French microcatheter (JB1 catheter, Cook Medical) enabled manipulation into the celiac axis followed by a celiac artery angiogram to delineate hepatic blood supply. Using digital subtraction angiography (DSA) and cone-beam CT angiography (C-arm, Allura Clarity FD20 8.2, Philips), a region of hypervascular blush located in the left liver lobe was identified as the tumor. A steerable guide wire (0.014 in. Transcend wire, Boston Scientific) was used to selectively catheterize the tumor-feeding artery, and final positioning of the catheter was confirmed with DSA.

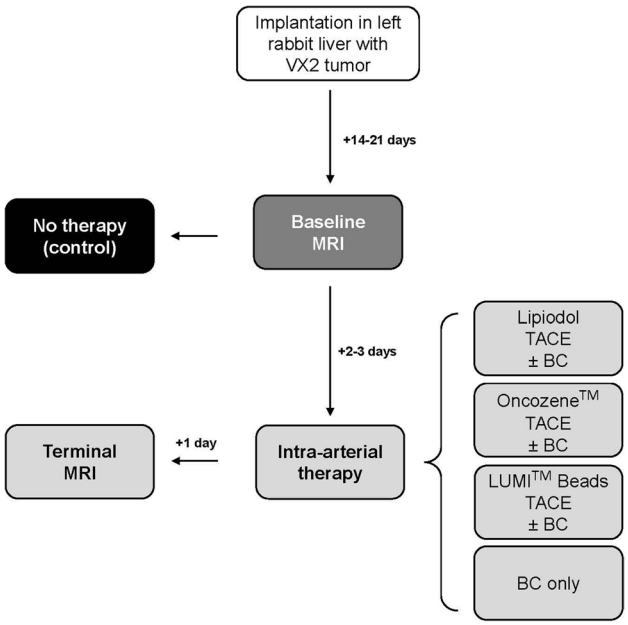

Fig. 1 Experimental in vivo study design. This flowchart illustrates the timeline of tumor implantation, imaging sessions, and therapy performed on experimental animals. The right column lists the different treatment options used

Conventional TACE

For rabbits undergoing cTACE, a Doxorubicin-Lipiodol emulsion was prepared immediately before intra-arterial injection. Briefly, 1.25 mg/mL of Doxorubicin HCl (Research Products International) was mixed 1:2 with Lipiodol (Guerbet) and stable formation of droplets was confirmed performing a drop test [23]. Depending on tumor size and blood supply, 0.2–0.3 mL of the Doxorubicin-Lipiodol emulsion was slowly infused via the tumor-feeding artery under fluoroscopy monitoring. Subsequently, the catheter was flushed with saline and 0.3–0.4 mL of 100–300 µm embolics (Embospheres, Merit Medical) mixed 1:4 with Omnipaque350 (Amersham Health) was administered until complete stasis was observed.

TACE with drug-eluting embolics

Previous to TACE with Idarubicin-eluting beads, 40-µm Oncozene™-microspheres were loaded with 15 mg of Idarubicin solution (Idamycin PFS™, Pfizer) according to manufacturer's instructions [24]. After removing any excess liquid, 7.5 mL Omnipaque contrast agent and 7.5 mL sterile water were added to 3 mL of loaded microsphere suspension. A volume of 0.3–0.5 mL of the mix was injected through the selectively placed catheter until complete stasis.

For TACE with 40–90-µm Doxorubicin-eluting beads, radiopaque LUMI™-beads were loaded with Doxorubicin HCl solution for 2 h under continuous mechanical agitation as previously described [25, 26]. The sedimented beads were then diluted with Omnipaque contrast agent to a final Doxorubicin concentration of 1.25 mg/mL. 0.2–0.4 mL of the suspension was injected in the tumor-feeding artery until complete stasis.

Bicarbonate infusion

In all animals receiving bicarbonate either directly prior to TACE or alone, 6 mL of a 1:1 mix of Omnipaque contrast agent and 4% sodium bicarbonate USP (Neut™, Hospira) was slowly injected as soon as the catheter was place in the hepatic artery and while advancing the catheter into the tumor-feeding artery. Once a selective positioning of the catheter was confirmed, 5 mL of the 4% bicarbonate solution was slowly injected over 5 min to prevent vasospasms. Afterwards, the catheter was flushed with saline prior to administration of chemotherapeutic or embolic agents in order to prevent clotting. We hypothesize that the consecutive application of embolizing agents leads to a trapping of bicarbonate in the tumor tissue and prevented its clearance.

Imaging protocol

MRI data was acquired on a 3-T MR scanner (Magnetom Prisma, Siemens) using a 15-channel knee RF coil prior to and—excluding controls—1 day after intra-arterial treatment. The imaging protocol included native and contrast-enhanced T_1-weighted using a 3D VIBE sequence with CAIPIRINHA (2×2) parallel imaging and respiratory-gated T_2-weighted spin echo and respiratory-gated diffusion-weighted echo planar imaging for reconstruction of apparent diffusion coefficient maps. Scan parameters were TR/TE/Θ = 3.45 ms/1.28 ms/9°, matrix 192×100, 6/8 partial Fourier, bandwidth 500 Hz/pix, FOV = 200×120 mm^2, 25–32 slices, 2–3 s/volume, and 1×2×2.5 mm^3. Before, during, and after the bolus injection of 0.1 mmol/kg intravenous gadolinium, eighty multi-slice volumes were run repeatedly. pH_e mapping with BIRDS was performed at the terminal MRI after infusion of 15 mL of $TmDOTP^{5-}$ (Macrocyclics) at a rate of 0.5 mL/min for 30 min for a total dose of 0.5 mmol/kg as previously described [13, 17]. BIRDS uses magnetic resonance spectroscopic imaging (MRSI) to directly detect paramagnetically shifted signals from non-exchangeable protons of complexes between lanthanide ions like thulium and macrocyclic chelates such as 1,4,7,10-tetraazacyclododecane-1,4,7,10-tetrakis (methylene phosphonate or $DOTP^{8-}$) [27, 28]. The short relaxation times of signals emanating from these complexes allow for ultrafast pH_e imaging. For BIRDS, we used a 3D MRSI sequence with a recycle time of 8 ms, a FOV of 20×20×25 cm^3, 20 averages, 13×13×13 rectangular encoding steps, 6-min total acquisition time, and reconstructed to 25×25×25 resolution, with a voxel size of 8×8×10 mm^3. The pH_e was calculated in each voxel using the H2, H3, and H6 signals of $TmDOTP^{5-}$ [27, 28]. The pH_e was obtained in a voxel-wise manner in both the tumor tissue and tumor-free liver, separately. For the investigation of pH_e in the tumor-free hepatic tissue, the liver was outlined to exclude the tumor tissue, gall bladder, and large hepatic vessels. The average pH_e was then calculated using the voxels from both contralateral and ipsilateral regions within this outlined area. Comparisons between groups were obtained with Mann–Whitney *U* test using Prism (v7.0; GraphPad) in a voxel-wise manner under the assumption that all voxels are independent from each other. This assumption is based on the fact that each voxel reflects a regional tumor characteristic containing a certain type of tissue with cells that behave in a certain way depending on their own environment but independent on the neighboring voxels, and which could be influenced by the treatment. We assumed that all cells in the same treatment group behave similarly under similar circumstances independent if they are in the same animal or in a different animal.

Immunohistological analysis

After animals were sacrificed by intravenous injection of euthasol (0.5 mL/kg), tumor tissue was harvested, fixated in 10% buffered formalin overnight, paraffin-embedded, and sectioned into slides of 5–8 µm. Histopathological characterization was correlated with imaging findings. Tumor necrosis was confirmed with hematoxylin/eosin (H&E) staining and further characterized by markers indicating cell viability and proliferation (PCNA Monoclonal Antibody, Thermo Fisher Scientific, catalog#MA5-11,355; dilution 1:400) as well as apoptosis (TUNEL Apoptosis Detection Kit, Millipore, Cat#17–141). Additionally, tumor sections were evaluated for markers of immune response, in which the presence of antigen-presenting cells (APC) and T-lymphocytes was investigated through IHC analysis using anti-HLA-DR (Cat#ab166777, Abcam; dilution 1:1000) and anti-CD3 (Cat#ab11089, Abcam; dilution 1:200), respectively. IHC staining results were analyzed qualitatively and quantitatively using Aperio ImageScope (v12.3.3.5048, Leica Biosystems) at ×20 magnification. As a computer-driven quantitative image analysis, percentage cell positivity was assessed with ImageScope v12.3 positive-pixel-count-algorithm using whole slide analysis versus selection of 2 mm^2 hot spot area in three representative field of views (×20 magnification) on one stained slide per rabbit and staining. A positivity index (PI) was calculated as percentage of positively stained cells of total cell count and is presented as mean of all analyzed representative regions. The PI was assessed separately for intratumoral or extratumoral areas and for both HLA-DR and CD3 stainings in each group.

Results

pH_e mapping reveals deacidification of TME following bicarbonate-enhanced cTACE

pH_e mapping with BIRDS was used to monitor therapy-induced changes of tumor pH_e. Examples of colored pH_e maps are shown in Fig. 2. To compare effects of different chemoembolic regimens, the average intratumoral pH_e value (Fig. 3a) and normal liver pH_e (Fig. 3b) were calculated in a voxel-wise manner for each TACE treatment. Results are depicted in Table 1. These measurements revealed significant acidosis of the tumor tissue in untreated controls as compared to liver parenchyma ($p < 0.0001$). The use of bicarbonate prior to cTACE was the only combination to significantly increase tumor pH_e 24 h after therapy compared to cTACE alone ($p = 0.0025$) and control ($p = 0.0175$). In contrast, cTACE alone ($p = 0.8763$), Oncozene™-TACE ($p = 0.3402$) and LUMI™-bead-TACE ($p = 0.8763$) administered alone or combined with bicarbonate ($p = 0.6485$ and $p = 0.8889$, respectively) did not reveal a significant modulating impact on pH_e as compared to

control. Although injection of sodium bicarbonate prior to DEE-TACE with LUMI™-beads was associated with a slight increase in pH_e as compared to LUMI™-beads alone ($p = 0.0952$), bicarbonate prior to Oncozene™-TACE did not modulate pH_e as compared to the use of Oncozenes™ alone ($p = 0.5209$). Local intra-arterial infusion of bicarbonate solution alone ($p = 0.3660$) did not show any ability to modulate pH_e when compared to control ($p = 0.3660$). Complete recovery of tumor pH_e to physiological conditions was not achieved with sodium bicarbonate, with tumor pH_e remaining lower than liver pH_e in all groups.

Impact of different chemoembolic materials on tumor viability

Qualitative analysis of histopathological PCNA indicated similar extent of immediate therapy-related inhibition of tumor cell proliferation in cTACE, Oncozene™-DEE-TACE, and LUMI™-DEE-TACE as compared to untreated control and intra-arterial bicarbonate infusion alone (Fig. 2, third row). TUNEL staining demonstrated equal therapy-induced tumor apoptosis and necrosis across all embolized tumors compared with little positive TUNEL staining in animals receiving no treatment or intra-arterial bicarbonate infusion only (Fig. 2, bottom row).

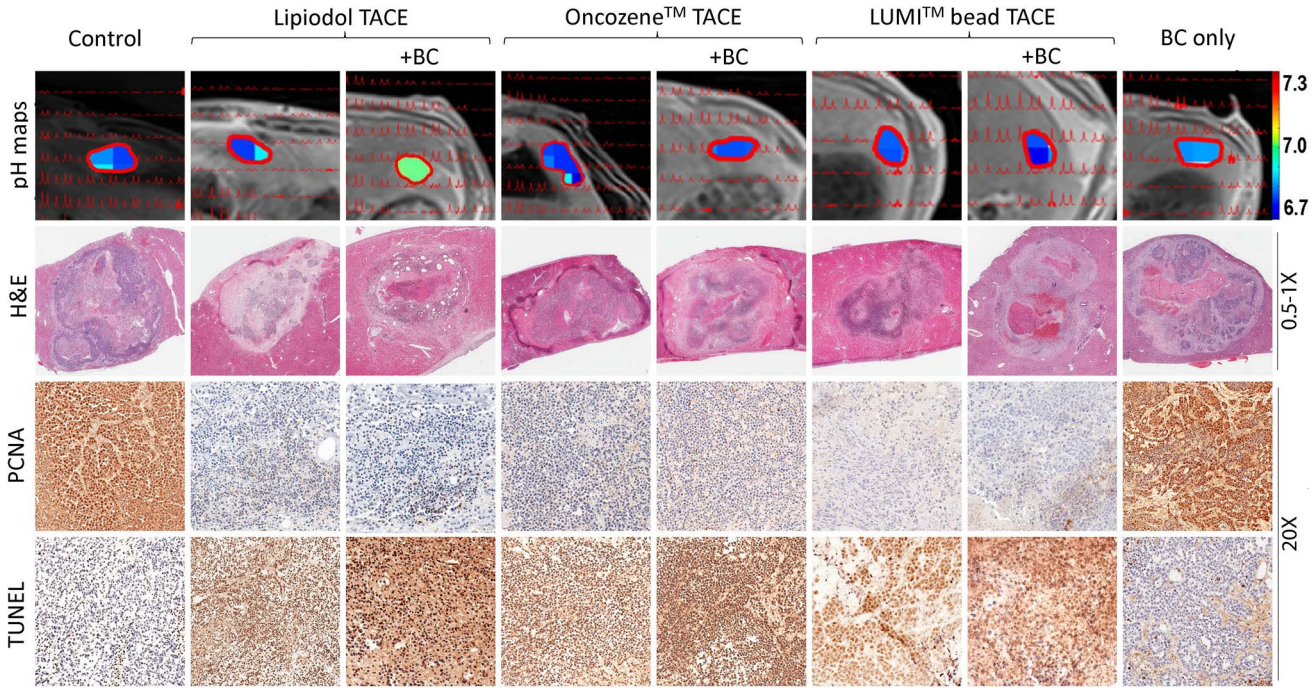

Fig. 2 Impact of different chemoembolic materials on tumor viability and extracellular pH. In the first row, examples of pH_e mapping with BIRDS are shown where MRSI data (red) and pH_e maps inside the tumors (outlined in red) were overlaid onto corresponding anatomical T_1-weighted MR images of one exemplary rabbit for each treatment group. Photomicrographs of hematoxylin–eosin (H&E)-stained tissue slides (second row) represent assessment of gross morphology. Exemplary regions in the tumor center of PCNA (third row) and TUNEL (fourth row)-stained specimens indicate evaluation of cell viability and necrosis, respectively

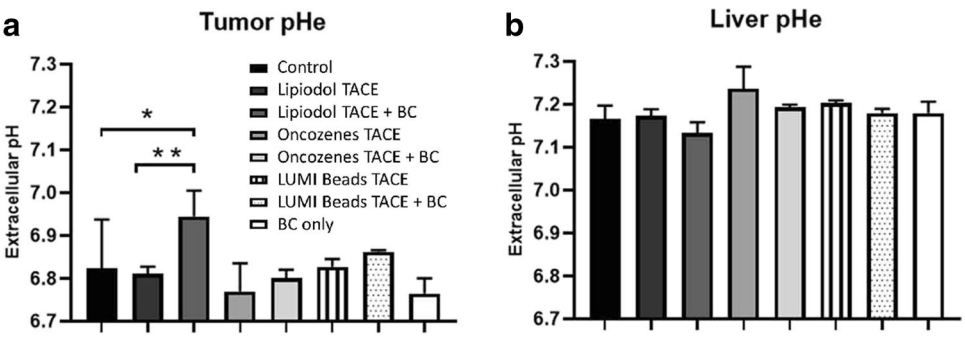

Fig. 3 pH_e measurements inside and outside the tumors. The average pH_e was calculated (**a**) inside the tumor and (**b**) surrounding, tumor-free liver parenchyma. The error bars represent the standard deviation for each treatment. Significant differences are indicated by * between the different treatment options (*$p \leq 0.05$; **$p \leq 0.01$)

Table 1 Extracellular pH in tumor tissue and liver parenchyma derived from pH mapping with BIRDS

	Control	cTACE		Oncozenes™		LUMI™-beads		BC only
			+BC		+BC		+BC	
Tumor pH_e(mean ± SD)	6.82 ± 0.11	6.81 ± 0.02	66.95 ± 0.05	6.77 ± 0.07	6.80 ± 0.02	6.83 ± 0.02	6.86 ± 0.01	6.76 ± 0.04
Liver pH_e(mean ± SD)	7.16 ± 0.06	7.18 ± 0.04	7.13 ± 0.05	7.24 ± 0.06	7.19 ± 0.02	7.20 ± 0.02	7.18 ± 0.03	7.18 ± 0.04

Immunohistochemistry staining

IHC staining of HLA-DR$^+$ APCs and CD3$^+$ T-lymphocytes revealed differences in immune-modulating effects on the TME across different treatment groups. Intratumoral (Fig. 4) and peritumoral (Fig. 5) regions were analyzed separately for the presence of HLA-DR$^+$ and CD3$^+$ cells and positivity indices were calculated for each group (Fig. 6).

Untreated tumor controls

In untreated controls, histological analysis revealed a lack of tumor-infiltrating APCs and T-lymphocytes. In contrast, about a third of peritumoral cells were either HLA-DR$^+$ or CD3$^+$.

An addition of bicarbonate infusion without further treatment did not strongly alter the immune cell profile intra- or peritumorally compared to controls.

cTACE without and with addition of bicarbonate

In cTACE-treated tumors, little intratumoral immune cell infiltration was noticed and peritumoral infiltration was diminished compared to controls. Combined bicarbonate-cTACE therapy restored intratumoral and especially peritumoral APC infiltration without a strong effect on T-cell infiltration.

DEE-TACE with Oncozenes™ without and with addition of bicarbonate

DEE-TACE using Oncozenes™ enabled moderate intratumoral recruitment of both APCs and T-lymphocytes. Peritumoral APC infiltration was predominant across all treatment groups with a positivity index of 90%, while T-lymphocyte accumulation was not increased as compared to controls. While the use of bicarbonate prior to Oncozene™-TACE did not favor intratumoral immune recruitment, the density of peritumoral APC infiltration was reduced without meaningful changes in overall CD3$^+$-cell distribution.

DEE-TACE with LUM™-beads without and with addition of bicarbonate

LUMI™-bead-TACE-treated tumors displayed moderate intratumoral immune cell infiltration with fewer immune

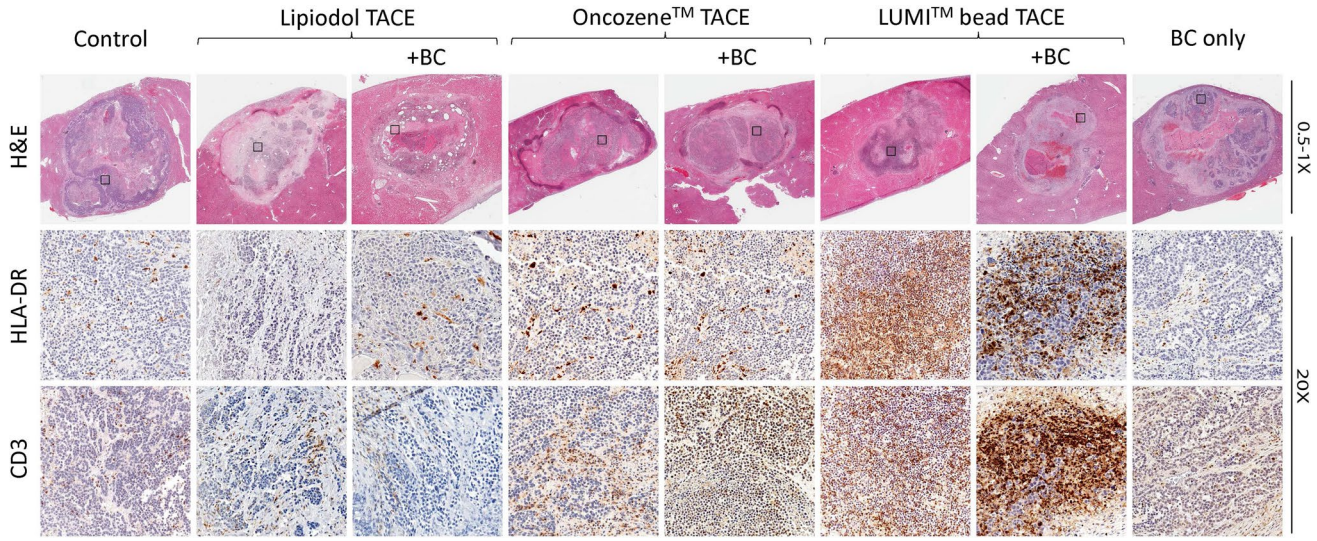

Fig. 4 Intratumoral distribution of immune cells across different treatment groups. Photomicrographs of H&E-stained slides (first row, ×0.5–1 magnification) indicate the area of ×20 magnification for IHC staining of HLA-DR (second row) and CD3 (third row) receptors across the different treatment and control groups. Intratumoral presence of HLA-DR$^+$ APCs and CD3$^+$ T-cells is moderate in untreated control and bicarbonate (BC) infusion only and cTACE-treated tumors, but enhanced in regimens using cTACE in combination with BC or DEE-TACE using Oncozenes™ or LUMI™-beads with or without BC. Strongest intratumoral presence of APCs and especially T-cells is seen when combining LUMI™-bead-TACE with BC

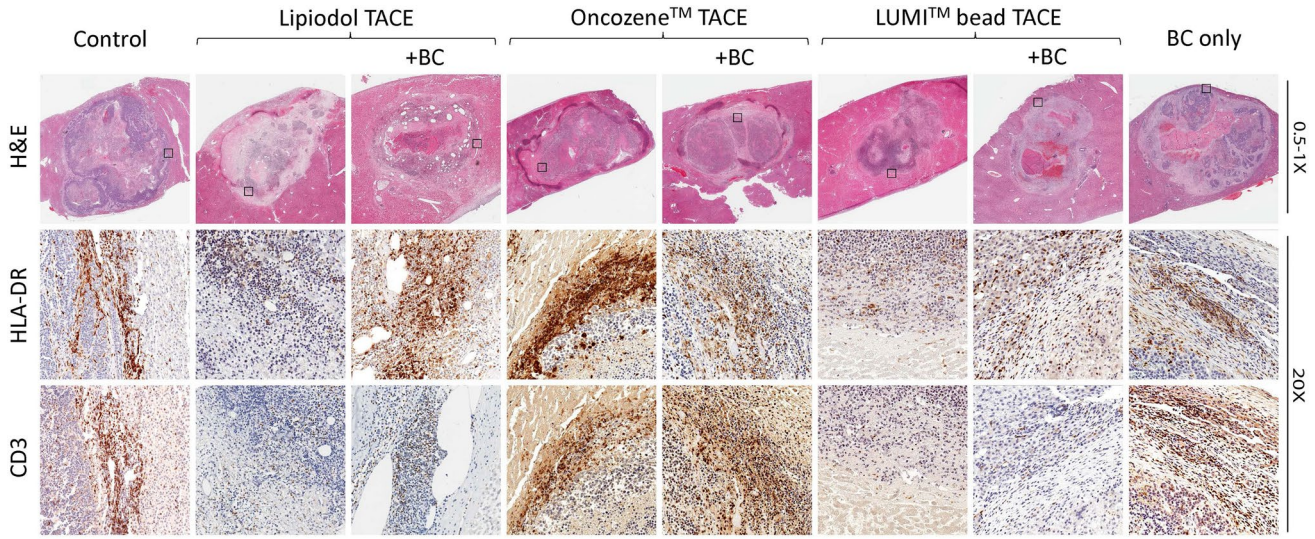

Fig. 5 Peritumoral distribution of immune cells across different treatment groups. Photomicrographs of H&E-stained specimens (first row, ×0.5–1) indicate the area of ×20 magnification for IHC staining of HLA-DR (second row) and CD3 (third row) receptors across the different treatment and control groups. Moderate peritumoral presence of both HLA-DR + APCs and $CD3^+$ T-cells is seen in untreated controls and tumors receiving bicarbonate (BC) infusion only, which disappeared after treatment with cTACE, but reappeared when bicarbonate infusion was added to cTACE. Marked dense peritumoral infiltration of especially APCs is seen in Oncozene™-treated rabbits, but slightly reduced after additional BC infusion without meaningful change in $CD3^+$ cell distribution. Peripheral accumulation of immune cells is sparse in LUMI™-TACE-treated tumors with and without additional BC infusion

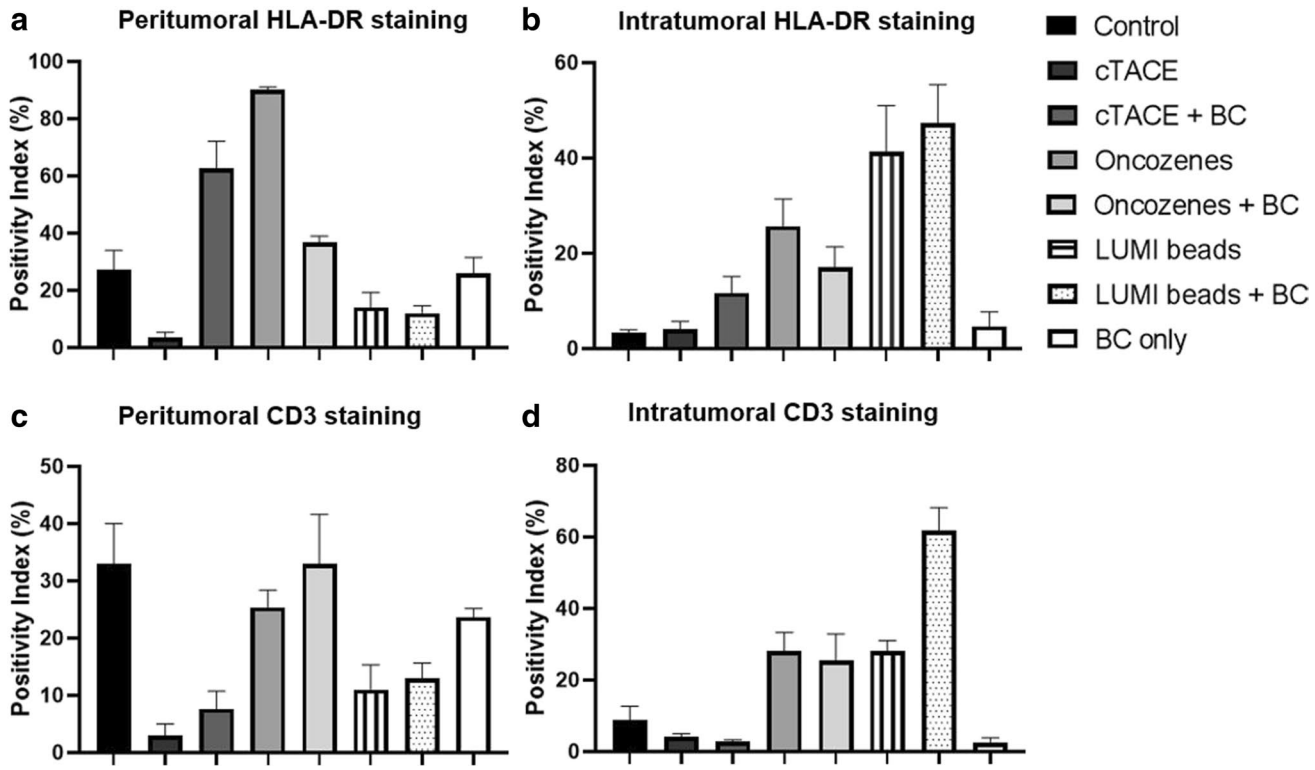

Fig. 6 Positivity indices of HLA-DR and CD3 stainings across all treatment groups. The average positivity index was calculated in both peritumoral tissue for (**a**) HLA-DR and (**c**) CD3 stained IHC slides and intratumoral tissue for (**b**) HLA-DR and (**d**) CD3-stained IHC slides. The error bars represent the standard deviation for each treatment group

cells being observed peritumorally. In contrast, prior bicarbonate therapy seemed to strongly modulate the effects of LUMI™-bead-TACE on both APC and T-cell infiltration intratumorally while not exerting any therapy-induced peritumoral cell recruitment.

Discussion

The presented results indicate that addition of bicarbonate to cTACE is the only across all tested combinations successfully normalizing tumor pH_e towards a higher, more physiological value. Furthermore, a key finding from IHC staining results is that different chemoembolic regimens result in different immune reactions manifesting in unequal accumulation and migration of APCs and T-lymphocytes in tumor tissue.

The tight relationship between metabolic characteristics and immune-evading mechanisms of cancer cells has been subject of recent discussions and investigations [15, 19, 29]. As previously described [19], untreated tumors are characterized by low pH_e, which can be significantly elevated by combined cTACE and pH-buffering therapy with sodium bicarbonate. However, similar effects were not observed when combining DEE-TACE with bicarbonate. A possible explanation may be a higher capacity of cTACE to capture and trap bicarbonate due to the subsequent administration of Lipiodol, which penetrates into small vessels and occludes the outflow tract, followed by microspheres obstructing larger inflow vessels. In contrast, DEEs may only embolize larger vessels of the inflow tract, potentially leading to bicarbonate washout through small vessels, which remain patent. Injection of bicarbonate alone did not modulate pH_e compared to control, suggesting that embolization with Lipiodol is a critical component to contain bicarbonate and allow it to exert its pH_e-modulating effect. The ability to monitor pH_e modulation in vivo is especially powerful due to the close link between metabolism and immune-evading mechanisms of tumor cells hampering beneficial treatment outcomes [15, 29]. Low pH_e has been proven to result in inhibition of T-cells [14] and monocyte migration [16], contributing to tumor immune evasion.

Consistent with previous work [13], histopathological analysis of control samples revealed immune cell recruitment only at the margins of untreated tumors, indicative of strong interdependence between TME acidity and immune cell infiltration. Accordingly, buffering pH_e through combined cTACE therapy and sodium bicarbonate re-established local immunopermissiveness as compared to cTACE alone.

These findings imply that in addition to pH_e modulation, the choice of the chemoembolic regimen itself can affect anti-tumor immune responses. After DEE-TACE with Oncozenes™, pH_e was the lowest across all treatment groups. Yet, moderate intratumoral immune infiltration was present and peritumoral immune accumulation was the strongest across all groups. A contributing factor may be the use of Idarubicin, which has a higher toxicity index towards HCC compared to Doxorubicin [30], possibly causing more aggressive tumor destruction unmasking shielded tumor-associated antigens to APCs, which set the ground for early immune activation and recruitment of T-cells [31]. Furthermore, a more distal embolization caused by the Oncozenes compared to Lipiodol may allow for remaining collateral and portal blood flow allowing immune cell migration and the non-resorbable, negatively charged hydrogel microspheres themselves may cause an innate immune reaction as foreign material to the body, more immunogenic than Lipiodol-Doxorubicin emulsion. This could also trigger HLA-DR expressing APCs such as macrophages and dendritic cells, which then engage cytotoxic T-cells [31]. Unlike cTACE, combining Oncozenes™ with bicarbonate did not further enhance local inflammatory response, which is congruent with pH_e mapping results showing no modulation of pH_e compared to Oncozenes™ alone.

Similar to DEE-TACE with Oncozenes™, treatment with LUMI™-beads led to moderate intratumoral presence of predominant APCs but also T-cells, supporting the hypothesis of immune response caused by microspheres themselves. In contrast to Oncozenes™, almost no peritumoral immune cell infiltration occurred with LUMI™-beads alone. When combined with bicarbonate, pH_e imaging showed a small but insignificant increase compared to LUMI™-TACE alone ($p = 0.0952$), implying an improved mechanism preventing bicarbonate washout using LUMI™-beads compared to Oncozenes™. Additional to its pH-modulating effect, in previous studies, bicarbonate has shown to enhance the inflammatory response through activation of signaling pathways in macrophages [32] and can increase the cellular uptake of Doxorubicin, resulting in improved therapeutic outcome and an increment of immune cells in the TME [33]. Overall, bicarbonate-adjacent LUMI™-bead-TACE showed the strongest intratumoral accumulation of APCs and T-lymphocytes across all regimens. The stable and constant release of the chemotherapeutic agent in LUMI™-bead-TACE compared to cTACE [34] might possibly lead to a prolonged necrotic effect and uncovering of tumor-antigens, and therefore, immune-cell recruitment as well as a prolonged weakening of immune evasion mechanism of the tumor might contribute to the ability of immune cells to migrate into the tumor. This intratumoral immune cell presence in direct contact with malignant cells is associated with prolonged survival and better response to immunotherapy [35, 36]. Hence, understanding the diverse immune-modulating effects of different TACE regimens is of clinical importance. The goal of immunotherapy is to boost patient's own anti-tumor immune response by rescuing impaired T-cell function and immune

surveillance [37]. HCC is an immunogenic tumor developing in an immune-suppressed environment, making it moderately susceptible to immunotherapies [38] and resulting in modest clinical improvement [39]. Recent investigations on VX2 tumor-bearing rabbits treated with local radiofrequency ablation demonstrated not only an upregulation of pro-inflammatory cytokines and increased antitumoral T-cell response but also improved prevention of tumor spread and survival after combination with TLR9 agonists [40]. Similar mechanism might appear in combination of TACE with immune-modulatory treatments. Thus, an investigation of cytokine levels and dynamics after TACE treatment especially when combined with immunotherapeutics is of great interest to further improve response rates in patients with advanced HCC and should be conducted in future studies.

Anticipation of greater efficiency of favorable immunological effects of TACE [20, 21] in combination with immunotherapy has provided a rationale to start several clinical trials combining TACE with nivolumab (NCT03143270, NCT03572582), pembrolizumab (NCT03397654), and many other immunotherapies [38]. To achieve maximal treatment effects, the choice of the chemoembolic regimen has to be deliberated as it can strongly enhance or inhibit the innate immune response, herein affecting response rates. Further experimental and clinical research on modifying effects of available materials on the TME is necessary.

A limitation of this study is the use of rabbits carrying a VX2 tumor of non-hepatic origin, lacking associated conditions often present in HCC such as cirrhosis. However, the VX2 liver tumor model is established for HCC animal studies and has shown to be fairly predictive of clinical outcomes [41, 42]. In general, there are limited options for TACE in animal models; therefore, the rabbit was chosen as a compromise for the purpose of this radiological-pathological study. Furthermore, the relatively low spatial resolution resulting from BIRDS imaging leaves room for improvement in future experiments which could be achieved by applying more efficient k-space sampling methods or increasing the signal-to-noise ratio using a more sensitive coil. Another limitation is the missing differentiation between CD4 + T-helper cells and cytotoxic CD8 + T-cells. During our experiments, we tried different anti-CD8 + and anti-CD4 + antibodies, but unfortunately none of them showed sufficient or specific staining. In general, many antibodies are not feasible for staining on rabbit tissue since rabbits are often used as hosts in antibody production and therefore strong background staining may appear.

Given the small sample size and short follow-up period, the benefits of combined metabolic and immunologic responses in HCC should be considered a proof-of-concept observation laying the groundwork for further investigation including longitudinal monitoring of immuno-metabolic changes. However, given that such multi-modal comparisons are difficult in clinical populations due to disease heterogeneity, some plausible conclusions about TACE with various embolic materials and chemotherapeutics can only be made in a preclinical study as shown here.

In conclusion, our findings indicate that there are notable differences in TME modulating effects between different chemoembolic regimens used for TACE. Several clinical studies combining intra-arterial therapies and immunotherapies are already ongoing. Taking immunogenic capacity of the different chemoembolic materials into consideration when designing future studies may augment the immune-enhancing abilities of immunotherapies and increase their response rates.

Acknowledgements We thank Christi Hawley, Marina Mammarian, Stephanie Thorne, Vasily Pekurovsky, and Jonathan Tefera for their support in animal care and handling.

Funding This study was supported by the following grants: NIH (R01 CA206180 and R01 EB023366) and the Society of Interventional Oncology (19–001324). Research reported in this article was also supported by the Yale Liver Center Microscopy Core. JW was supported in part by T32GM-007205 (Yale MSTP).

Declarations

Guarantor The scientific guarantor of this study is Julius Chapiro, MD.

Conflict of interest The co-author MingDe Lin is a Visage Imaging, Inc., employee and stock holder. MingDe Lin is an Executive Councilor for Tau Beta Pi Association, Inc.
The other authors declare no competing interests.

Statistics and biometry Lawrence Staib, PhD, Yale School of Medicine, and Dr. rer. nat. Konrad Neumann, Institute for Biometry and Clinical Epidiomology of the Charite Universitätsmedizin Berlin, kindly provided statistical advice for this manuscript.

Informed consent Approval from the institutional animal care committee was obtained.

Ethical approval Institutional Review Board approval was not required because no patients were included in this study.

Study subjects or cohorts overlap Data from a subgroup of animals were used for a published poster "Characterization of liver tumor microenvironment after treatment with different embolic materials using non-invasive molecular imaging of extracellular pH" on the conference of the Society of Interventional Oncology in 2020. Furthermore, data derived from experiments with a subset of animals ($n = 12$) were used in previous publications "Molecular Imaging of Extracellular Tumor pH to Reveal Effects of Locoregional Therapy on Liver Cancer Microenvironment" by Savic LJ, Schobert IT, Peters D, et al. published in Clinical Cancer Research in 2020 and "Molecular MRI of the Immuno-Metabolic Interplay in a Rabbit Liver Tumor Model: A Biomarker for Resistance Mechanisms in Tumor-targeted Therapy?" by Savic LJ, Doemel LA, Schobert IT, et al. published in Radiology in 2020.

Methodology
- Experimental
- Performed at one institution

References

1. Bray F, Ferlay J, Soerjomataram I et al (2018) Global cancer statistics 2018: GLOBOCAN estimates of incidence and mortality worldwide for 36 cancers in 185 countries. CA Cancer J Clin 68:394–424. https://doi.org/10.3322/caac.21492
2. Dimitroulis D, Damaskos C, Valsami S et al (2017) From diagnosis to treatment of hepatocellular carcinoma: an epidemic problem for both developed and developing world. World J Gastroenterol 23:5282–5294. https://doi.org/10.3748/wjg.v23.i29.5282
3. Forner A, Reig ME, Rodriguez de Lope C, Bruix J (2010) Current strategy for staging and treatment: the BCLC update and future prospects. Semin Liver Dis 30:061–074. https://doi.org/10.1055/s-0030-1247133
4. Llovet JM, Bruix J (2003) Systematic review of randomized trials for unresectable hepatocellular carcinoma: chemoembolization improves survival. Hepatology 37:429–442. https://doi.org/10.1053/jhep.2003.50047
5. Lee H-S, Kim KM, Yoon J-H et al (2002) Therapeutic efficacy of transcatheter arterial chemoembolization as compared with hepatic resection in hepatocellular carcinoma patients with compensated liver function in a hepatitis B virus-endemic area: a prospective cohort study. J Clin Oncol 20:4459–4465. https://doi.org/10.1200/JCO.2002.02.013
6. Llovet JM, Real MI, Montaña X et al (2002) Arterial embolisation or chemoembolisation versus symptomatic treatment in patients with unresectable hepatocellular carcinoma: a randomised controlled trial. Lancet 359:1734–1739. https://doi.org/10.1016/S0140-6736(02)08649-X
7. Lencioni R (2010) Loco-regional treatment of hepatocellular carcinoma. Hepatology 52:762–773. https://doi.org/10.1002/hep.23725
8. Zou JH, Zhang L, Ren ZG, Ye SL (2016) Efficacy and safety of cTACE versus DEB-TACE in patients with hepatocellular carcinoma: a meta-analysis. J Dig Dis 17:510–517. https://doi.org/10.1111/1751-2980.12380
9. Varela M, Real MI, Burrel M et al (2007) Chemoembolization of hepatocellular carcinoma with drug eluting beads: efficacy and doxorubicin pharmacokinetics. J Hepatol 46:474–481. https://doi.org/10.1016/j.jhep.2006.10.020
10. Marelli L, Stigliano R, Triantos C et al (2007) Transarterial therapy for hepatocellular carcinoma: which technique is more effective? A systematic review of cohort and randomized studies. Cardiovasc Intervent Radiol 30:6–25. https://doi.org/10.1007/s00270-006-0062-3
11. Sacco R, Bargellini I, Bertini M et al (2011) Conventional versus doxorubicin-eluting bead transarterial chemoembolization for hepatocellular carcinoma. J Vasc Interv Radiol 22:1545–1552. https://doi.org/10.1016/j.jvir.2011.07.002
12. Lammer J, Malagari K, Vogl T et al (2010) Prospective randomized study of doxorubicin-eluting-bead embolization in the treatment of hepatocellular carcinoma: results of the PRECISION V study. Cardiovasc Intervent Radiol 33:41–52. https://doi.org/10.1007/s00270-009-9711-7
13. Savic LJ, Schobert IT, Peters D et al (2020) Molecular imaging of extracellular tumor pH to reveal effects of locoregional therapy on liver cancer microenvironment. Clin Cancer Res 26:428–438. https://doi.org/10.1158/1078-0432.CCR-19-1702
14. Fischer K, Hoffmann P, Voelkl S et al (2007) Inhibitory effect of tumor cell–derived lactic acid on human T cells. Blood 109:3812–3819. https://doi.org/10.1182/blood-2006-07-035972
15. Huber V, Camisaschi C, Berzi A et al (2017) Cancer acidity: an ultimate frontier of tumor immune escape and a novel target of immunomodulation. Semin Cancer Biol 43:74–89. https://doi.org/10.1016/j.semcancer.2017.03.001
16. Goetze K, Walenta S, Ksiazkiewicz M et al (2011) Lactate enhances motility of tumor cells and inhibits monocyte migration and cytokine release. Int J Oncol 39:453–463. https://doi.org/10.3892/ijo.2011.1055
17. Coman D, Peters DC, Walsh JJ et al (2020) Extracellular pH mapping of liver cancer on a clinical 3T MRI scanner. Magn Reson Med 83:1553–1564. https://doi.org/10.1002/mrm.28035
18. Rao JU, Coman D, Walsh JJ et al (2017) Temozolomide arrests glioma growth and normalizes intratumoral extracellular pH. Sci Rep 7:7865. https://doi.org/10.1038/s41598-017-07609-7
19. Savic LJ, Doemel LA, Schobert IT, et al (2020) Molecular MRI of the immuno-metabolic interplay in a rabbit liver tumor model: a biomarker for resistance mechanisms in tumor-targeted therapy? Radiology 296(3):575–583. https://doi.org/10.1148/radiol.2020200373
20. Ayaru L, Pereira SP, Alisa A et al (1950) (2007) Unmasking of alpha-fetoprotein-specific CD4(+) T cell responses in hepatocellular carcinoma patients undergoing embolization. J Immunol Baltim Md 178:1914–1922. https://doi.org/10.4049/jimmunol.178.3.1914
21. Mizukoshi E, Nakamoto Y, Arai K et al (2011) Comparative analysis of various tumor-associated antigen-specific t-cell responses in patients with hepatocellular carcinoma. Hepatology 53:1206–1216. https://doi.org/10.1002/hep.24149
22. Flecken T, Schmidt N, Hild S et al (2014) Immunodominance and functional alterations of tumor-associated antigen-specific CD8+ T-cell responses in hepatocellular carcinoma. Hepatology 59:1415–1426. https://doi.org/10.1002/hep.26731
23. Deschamps F, Moine L, Isoardo T et al (2017) Parameters for stable water-in-oil lipiodol emulsion for liver trans-arterial chemoembolization. Cardiovasc Intervent Radiol 40:1927–1932. https://doi.org/10.1007/s00270-017-1763-5
24. LAS0049–01-TANDEM-Loading-Guidance-OUS-08.21.2013.pdf.pdf
25. Gaba RC, Emmadi R, Parvinian A, Casadaban LC (2016) Correlation of doxorubicin delivery and tumor necrosis after drug-eluting bead transarterial chemoembolization of rabbit VX2 liver tumors. Radiology 280:752–761. https://doi.org/10.1148/radiol.2016152099
26. Levy EB, Krishnasamy VP, Lewis AL et al (2016) First human experience with directly image-able iodinated embolization microbeads. Cardiovasc Intervent Radiol 39:1177–1186. https://doi.org/10.1007/s00270-016-1364-8
27. Coman D, Trubel HK, Rycyna RE, Hyder F (2009) Brain temperature and pH measured by 1H chemical shift imaging of a thulium agent. NMR Biomed 22:229–239. https://doi.org/10.1002/nbm.1312
28. Coman D, Trubel HK, Hyder F (2010) Brain temperature by Biosensor Imaging of Redundant Deviation in Shifts (BIRDS): comparison between TmDOTP5− and TmDOTMA−. NMR Biomed 23:277–285. https://doi.org/10.1002/nbm.1461
29. Buck MD, Sowell RT, Kaech SM, Pearce EL (2017) Metabolic instruction of immunity. Cell 169:570–586. https://doi.org/10.1016/j.cell.2017.04.004
30. Boulin M, Guiu S, Chauffert B et al (2011) Screening of anticancer drugs for chemoembolization of hepatocellular carcinoma. Anticancer Drugs 22:741–748. https://doi.org/10.1097/CAD.0b013e328346a0c5
31. Broz ML, Binnewies M, Boldajipour B et al (2014) Dissecting the tumor myeloid compartment reveals rare activating antigen-presenting cells critical for T cell immunity. Cancer Cell 26:638–652. https://doi.org/10.1016/j.ccell.2014.09.007
32. Kawakami T, Koike A, Maehara T et al (2020) Bicarbonate enhances the inflammatory response by activating JAK/STAT signalling in LPS + IFN-γ-stimulated macrophages. J Biochem 167:623–631. https://doi.org/10.1093/jb/mvaa010

33. Abumanhal-Masarweh H, Koren L, Zinger A et al (2019) Sodium bicarbonate nanoparticles modulate the tumor pH and enhance the cellular uptake of doxorubicin. J Control Release 296:1–13. https://doi.org/10.1016/j.jconrel.2019.01.004
34. Lewis AL, Gonzalez MV, Lloyd AW et al (2006) DC bead: in vitro characterization of a drug-delivery device for transarterial chemoembolization. J Vasc Interv Radiol 17:335–342. https://doi.org/10.1097/01.RVI.0000195323.46152.B3
35. Schmidt N, Thimme R (2016) Role of immunity in pathogenesis and treatment of hepatocellular carcinoma. Dig Dis 34:429–437. https://doi.org/10.1159/000444558
36. Herbst RS, Soria J-C, Kowanetz M et al (2014) Predictive correlates of response to the anti-PD-L1 antibody MPDL3280A in cancer patients. Nature 515:563–567. https://doi.org/10.1038/nature14011
37. Erinjeri JP, Fine GC, Adema GJ et al (2019) Immunotherapy and the interventional oncologist: challenges and opportunities—a society of interventional oncology white paper. Radiology 292:25–34. https://doi.org/10.1148/radiol.2019182326
38. Singh P, Toom S, Avula A et al (2020) The immune modulation effect of locoregional therapies and its potential synergy with immunotherapy in hepatocellular carcinoma. J Hepatocell Carcinoma 7:11–17. https://doi.org/10.2147/JHC.S187121
39. El-Khoueiry AB, Sangro B, Yau T et al (2017) Nivolumab in patients with advanced hepatocellular carcinoma (CheckMate 040): an open-label, non-comparative, phase 1/2 dose escalation and expansion trial. Lancet 389:2492–2502. https://doi.org/10.1016/S0140-6736(17)31046-2
40. Behm B, Fazio PD, Michl P et al (2016) Additive antitumour response to the rabbit VX2 hepatoma by combined radio frequency ablation and toll like receptor 9 stimulation. Gut 65:134–143. https://doi.org/10.1136/gutjnl-2014-308286
41. van Breugel JMM, Geschwind J-F, Mirpour S et al (2019) Theranostic application of lipiodol for transarterial chemoembolization in a VX2 rabbit liver tumor model. Theranostics 9:3674–3686. https://doi.org/10.7150/thno.32943
42. Borde T, Laage Gaupp F, Geschwind J-F et al (2020) Idarubicin-loaded ONCOZENE drug-eluting bead chemoembolization in a rabbit liver tumor model: investigating safety, therapeutic efficacy, and effects on tumor microenvironment. J Vasc Interv Radiol 31:1706-1716.e1. https://doi.org/10.1016/j.jvir.2020.04.010

Authors and Affiliations

Luzie A. Doemel[1,2] · Jessica G. Santana[1] · Lynn J. Savic[1,2,3] · Fabian M. Laage Gaupp[1] · Tabea Borde[1,4] · Alexandra Petukhova-Greenstein[1,2] · Ahmet S. Kucukkaya[1,2] · Isabel T. Schobert[1,2] · Charlie A. Hamm[2,5] · Bernhard Gebauer[2] · John J. Walsh[6] · Irvin Rexha[1,2] · Fahmeed Hyder[1,6,7] · MingDe Lin[1,8] · David C. Madoff[1,7,9,10,11] · Todd Schlachter[1] · Julius Chapiro[1,7] · Daniel Coman[1,7]

✉ Julius Chapiro
j.chapiro@googlemail.com

[1] Department of Radiology and Biomedical Imaging, Yale School of Medicine, 333 Cedar Street, New Haven, CT 06510, USA

[2] Department of Diagnostic and Interventional Radiology, Charité-Universitätsmedizin Berlin, corporate member of Freie Universität Berlin, Humboldt-Universität, and Berlin Institute of Health, 10117 Berlin, Germany

[3] Berlin Institute of Health, 10178 Berlin, Germany

[4] Department of Diagnostic and Interventional Radiology, Klinikum Rechts Der Isar, Technische Universitat München, Munich, Germany

[5] Institute for Diagnostic Radiology and Neuroradiology, Greifswald University Hospital, Ferdinand-Sauerbruch-Stras se, 17475 Greifswald, Germany

[6] Department of Biomedical Engineering, School of Engineering & Applied Science, 17 Hillhouse Avenue, New Haven, CT 06510, USA

[7] Yale Cancer Center, Yale School of Medicine, 333 Cedar Street, New Haven, CT 06510, USA

[8] Visage Imaging, Inc., San Diego, CA 92130, USA

[9] Division of Medical Oncology, Department of Medicine, Yale School of Medicine, New Haven, CT 06510, USA

[10] Yale Liver Center, Yale University School of Medicine, 333 Cedar Street, New Haven, CT 06510, USA

[11] Smilow Cancer Hospital Care Center - North Haven, 6 Devine Street, Fl 2, North Haven, CT 06473, USA